# Heavy neutron rich nuclei: production and investigation

IOP Conf. Series: Journal of Physics: Conf. Series **1023** (2018) 012004 doi:10.1088/1742-6596/1023/1/012004

# Heavy neutron rich nuclei: production and investigation

**S Zemlyanoy[1], K Avvakumov[1], N Kazarinov[1], V Fedosseev[2], R Bark[3], Z Blazczak[4] and Z Janas[5]**
[1]Joint Institute for Nuclear Research, Dubna 141980, Russia
[2]CERN, Switzerland
[3]iThemba LABS, Nat. Research Foundation, South Africa
[4]Faculty of Physics, A. Mickiewicz University, Umultowska 85, 61-614 Poznan, Poland
[5]Faculty of Physics, University of Warsaw, Hoza 69, PL-00681 Warsaw, Poland

E-mail: zemlya@jinr.ru

**Abstact.** For production and investigation of heavy neutron rich nuclei devoted the new setup, which is under construction at Flerov Laboratory for Nuclear Reactions (FLNR) - JINR, Dubna now. This setup is planned to exploit available beams from the U-400M cyclotron in low energy multi-nucleon transfer reactions to study exotic neutron-rich nuclei located in the "north-east" region of nuclear map. Products from 4.5 to 9 MeV/nucleon heavy-ion collisions, such as $^{136}$Xe on $^{208}$Pb, are to be captured in a gas cell and selectively laser-ionized in a sextupole (quadrupole) ion guide extraction system.

PACS: 25.60.Je, 28.60.+s, 42.62.Fi

## 1. Introduction

In order to produce and study multinucleon transfer reaction products the GAs cell based Laser ionization an Separation setup (GALS) is designed at Flerov Laboratory for Nuclear Reactions (JINR). This setup is intended for production of heavy nuclei from the north-east part of nuclear map – near to or above the magic neutron number $N = 126$. At last years [1-5] heavy neutron-rich nuclides are of great interest for nuclear astrophysics. This becomes obvious when one looks at the predicted path for r-process nuclei and their decay (see Fig. 1 in [1] and [2]). In addition, study of the nuclear structure of extremely neutron rich nuclei is important for the basic nuclear spectroscopy. New information can be obtained about the changes of nuclear ground state properties, e.g. appearance of new or disappearance of the classical magic numbers (as in the case of light neutron-rich nuclei) as well as the occurrence of rapid nuclear structural changes, due to sudden onset of collectivity.

It should be noted that the region of heavy neutron rich nuclei along the neutron line $N = 126$ is still a blank field of the nuclide chart. Recently new isotopes were unambiguously identified in reactions with a $^{238}$U beam impinging on a Be target at 1 GeV/nucleon [6]. The production cross-section for the new isotopes has been measured down to the pico-barn level and compared with predictions of different model calculations. Nevertheless the magic neutron number $N = 126$ for atoms with $Z = 75$ - 78 is as yet not achieved. This is because production and study of heavier neutron rich nuclei with $A > 160$ encounters both physical and technical problems (for details see [1, 4]). The production of neutron-rich heavy and superheavy nuclei using low-energy multinucleon transfer

reactions has been discussed by Zagrebaev and Greiner [4]. The high predicted yield, shown in Fig. 1, opens a new opportunity in the studies at heavy ion facilities**.**

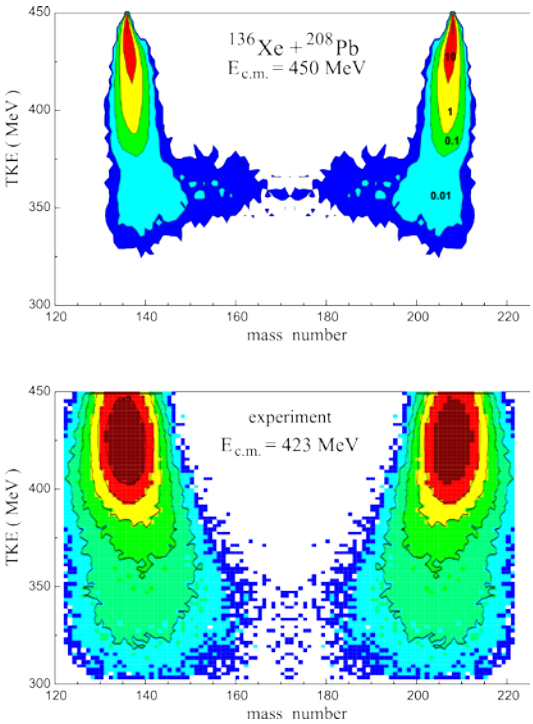


**Figure. 1** Dependence of the products yield of transfer reactions on the total kinetic energy and mass number**.** The figure compares the theoretical predictions of [4] (above) and the experimental results (below) from the JINR cyclotron U-400M (courtesy of V. Zagrebaev and E. Kozulin). The numbers in the right-hand side of the theoretical predictions present the cross-section in mb.

## 2. Experimental techniques

The experimental technique is already described in detail in [1-3, 7, 8]. Here we present only a brief,

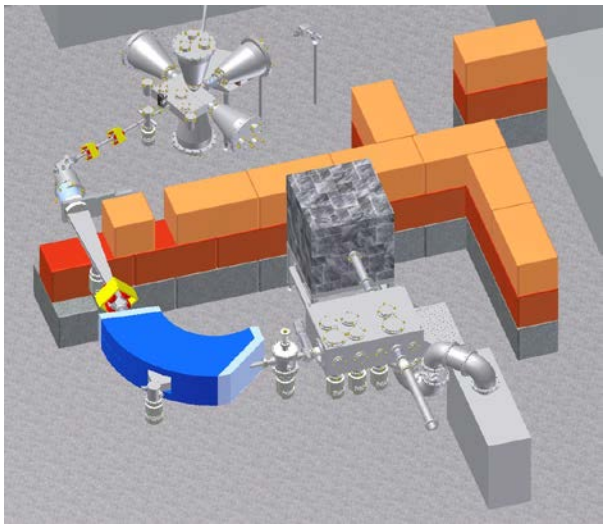

**Figure 2.** The allocation of the whole GALS facility in experimental cave near the hall of the cyclotron U-400M is shown in real scale.

overview of the experimental method that the GALS setup will use. The method, as proposed and applied in [7, 8], combines simultaneous *Z* and *A* separation based on stopping nuclei in gas cellsubsequent resonance laser ionization and mass-separation. The scheme of the GALS facility can be found in [3].

The operation principle is described in a number of papers (see e.g. [9] and the references therein). The first stage of laser system based on three Syra dye lasers pumped by two EgewaveYAG lasers and laser lab preparatory is almost finished. Now we concentrate on the GALS subsystems, located in the cave of Cyclotron U-400M experimental hall. Fig. 2 presents how these subsystems (Front-End, Enzel lenz, mass-separator, focal chamber and registration system) of GALS setup looks like. These subsystems are now in the advanced stage of realization. Mass separator could be a standard magnet separator similar to GPS at ISOLDE II [2, 10]) but nevertheless substantial efforts are needed for its realization. The same refers to the ion extraction and gas purification systems.

3D simulation of the beam dynamics in the GALS mass-separator was carried out in [11]. This simulation used 3D map of the AM magnetic field calculated using OPERA 3D code [12]. The number of particles used in this simulation was equal to 2 $10^4$. The computational model of the analyzing magnet is shown in Fig. 3.

**Figure 3.** Computational model of the analyzing magnet

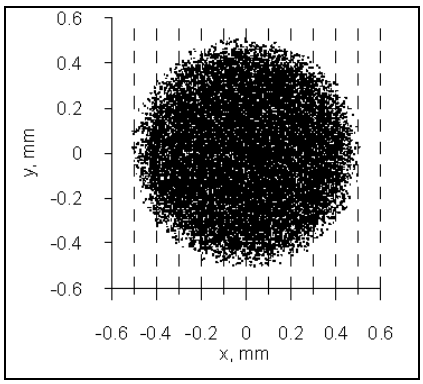


**Figure 4.** Initial particle distribution in plane {x,y}

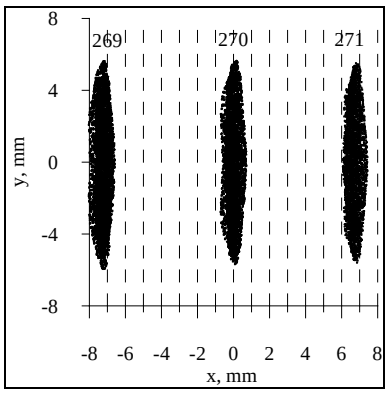


**Figure 5.** Ion distribution in the magnet focal plane

Fig. 6 shows the calculated distribution of the particles in the analysing magnet focal plane for the ions with A=269, 270, and 271. The estimated mass resolution of the spectrometer $R_m$ = 1400.

### 3. The ion guide simulation

The GALS front end vacuum chamber is designed to be used with different types of gas cells, the experiments will be started with the dual chamber gas cell (Fig. 6), and a horn-type gas cell is planned

to be used later for better evacuation efficiency of atoms of interest and for the experiments with in-gas-jet ionization [13]. The second option means that an S- or L-shaped segmented ion guide could be used in the gas cell chamber, so there should be enough space for it. Thus, the distance between the cyclotron beam and the extraction electrode is quite long (approximately 740 mm). On the first stage of the GALS setup a single long (about 630 mm) sextupole ion guide (SPIG) is planned to be used for guiding the ion beam from the gas cell to the extraction and acceleration electrostatics. In order to estimate possible losses of the ions interacting with the gas jet and background gas the simulations of the system containing the gas cell exit and the SPIG were carried out.

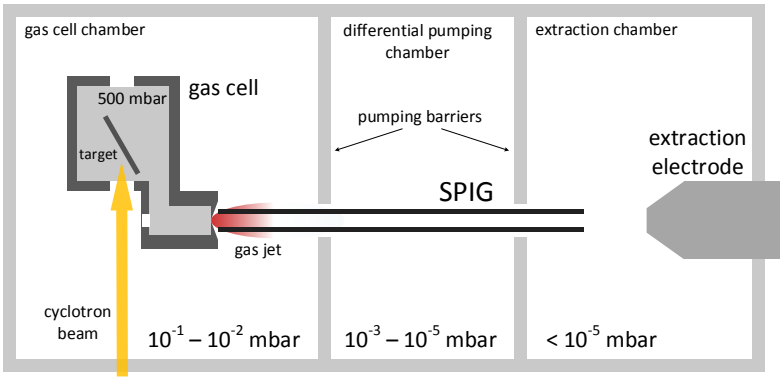


**Figure 6.** A schematic layout of GALS front-end.

Properties of a supersonic jet in a gas expansion from a gas cell to a vacuum chamber through a round orifice were discussed in detail in [14]. The simulations have been performed in the SIMION software package [15] using the hard sphere collision model and the additional code describing the gas jet [16]. In the model, the thermal ions propagate in a filled-cone direction distribution of half angle 30° out of the gas cell orifice, which has a diameter of 0.5 mm. The SPIG with an inner diameter of 3 mm consists of six rods (with a diameter of 1.5 mm and 630 mm long) cylindrically mounted on a sextupole structure, the distance from the orifice was set to 2 mm. The radiofrequency (4.7 MHz) voltage with peak-to-peak amplitude of 300 V is applied to the neighboring rods in the opposite phase, and the whole SPIG has a voltage of –210 V compared to the gas cell [17]. The pressure of gas (argon) was set to 500 mbar in the gas cell, $2 \cdot 10^{-2}$ mbar in the gas cell chamber, $2 \cdot 10^{-4}$ mbar in the differential pumping chamber and $2 \cdot 10^{-6}$ mbar in the extraction chamber.

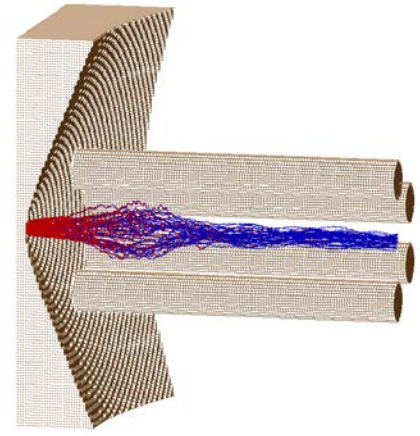

**Figure 7.** Simulated trajectories of the ions at SPIG entrance. The collisions with the buffer gas are marked with red

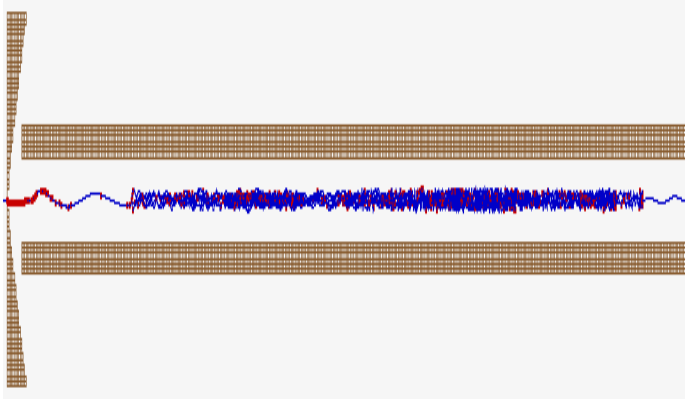

**Figure 8.** A trajectory of a single ion caught by a buffer gas inside the SPIG

Due to the simulations, almost no losses occur at SPIG entrance, but when the ions proceed from the gas jet to the background, they quickly lose most of the kinetic energy, which lead to high losses or at least very high time of flight. The trajectories of the ions interacting with the gas jet at the SPIG entrance are shown on Fig. 7. The ions' mean time of flight, mean longitudinal kinetic energy $KE_x$, their energy dispersion $\sigma_{KEx}$ and SPIG efficiency depending on the distance from the gas cell to the skimmer between the first and second cameras of the vacuum chamber are shown in Table 1, statistics of 200 ions used for each case, the ions' parameters were captured at the end of SPIG. As one can see when the distance is higher than 60 mm, the time of flight rises drastically, with decreasing of the kinetic energy along the beam axis. At such distances, the ions are being caught by buffer gas and it takes them about 5 ms or longer to diffuse to the SPIG exit, which is comparable with the time of evacuation from the gas cell. Fig. 8 represents an example a trajectory of such an ion inside the SPIG. The other option is losing such ions in collisions with the SPIG rods, but as the simulations show, the probability of this is rather low.

Based on the simulations results, one could assume the distances up to 60 mm to be acceptable for using experimentally, but the model used in the simulations does not describe in detail the slow pressure change in the skimmer aperture area, which means that experimental energy losses should be higher than indicated in the table. Thus, obtaining maximal efficiency and minimal time of flight is expected in case of skimmer location of 45-50 mm from the gas cell. These results are planned to be tested by further calculations and experiments.

Table 1. The parameters of the ions at the end of SPIG in dependence of the distance between the skimmer and the gas cell

| Distance from the gas cell to the skimmer | Mean time of flight, μs | Mean longitudinal kinetic energy $KE_x$, eV | Longitudinal kinetic energy dispersion $\sigma_{KEx}$, eV | Efficiency, % |
|---|---|---|---|---|
| 40 mm | 1182.8 | 0.3031 | 0.1264 | 99 |
| 45 mm | 1220.6 | 0.2901 | 0.1140 | 100 |
| 50 mm | 1187.8 | 0.2980 | 0.1164 | 99.5 |
| 55 mm | 1246.6 | 0.2935 | 0.1074 | 99.5 |
| 60 mm | 1192.7 | 0.2986 | 0.1008 | 99.5 |
| 65 mm | 6747.3 | 0.0497 | 0.0515 | 99 |
| 70 mm | 9417.6 | 0.0394 | 0.0581 | 95 |

## 4. Planned experiments

We plan to perform the first online test on Os I. As already shown in [6], Os is very perspective candidate to achieve the neutron magic line $N = 126$. The last calculations of A.V. Karpov [15] predicted sufficiently high reaction cross section for Os isotope even above this magic line.

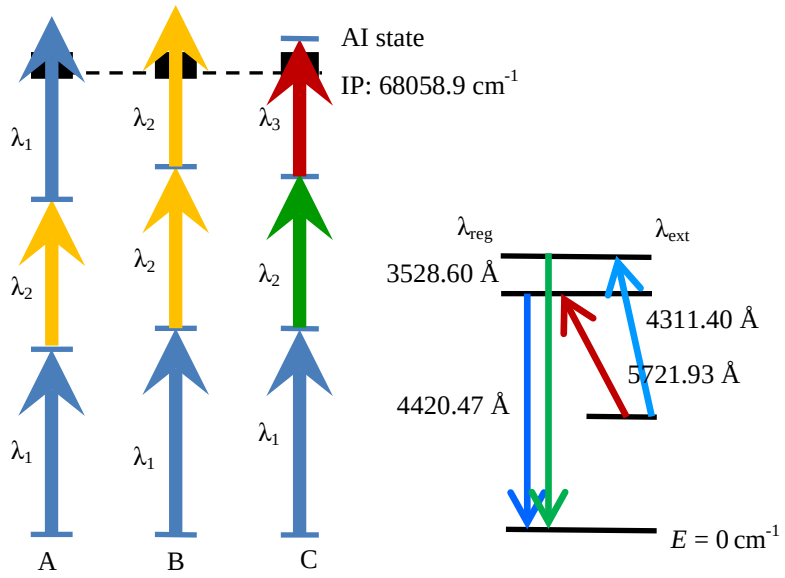


**Fig. 9** *Left*: possible ionization schemes of Os I (the wavelengths (in air) A: $\lambda_1$ = 3267.94Å $\lambda_2$ = 5509.33Å, B: $\lambda_1$ = 3018.04Å $\lambda_2$ = 5580.66Å, C[20]: $\lambda_1$ = 2909.06Å $\lambda_2$ = 4752.16Å $\lambda_3$ = 6043.15Å). *Right*: transitions for the off-line test experiments

Many spectroscopic data of Os I have been studied to find appropriate two- or three-steps transitions for laser ionization. Although there are many observed spectral lines as yet the atomic spectra information is not complete: most of the transitions are not assigned [16 - 19] and the atomic strengths are not known. Nevertheless several of the possible RIS scheme for Os have been previously studied [20, 21]. Three of them that seem to be more effective (see e.g. [21]) are shown in Fig. 9. The most ionization schemes are two colored three steps, the 3rd step being non-resonant.

By the end of 2018 off-line experiments with Os I will be started. Their aim is to check the quality of the reference cell using excitation and registration with different wavelengths (see right hand side of Fig. 7).

The most favorable ionization scheme is expected to be the resonance three steps one via an auto-ionizing state. At present no literature information is available about such states except the one at 71032 cm$^{-1}$ corresponding to the third step of case C [20]. For this reason at the second stage of the GALS activities a search for auto-ionizing states is planned. At the next phase of experiments an offline study of the optimal ionization scheme will be conducted. It supposes a detailed experimental study the efficiency of the different ionization schemes.

## 5. Conclusion

A new GALS facility at FLNR cyclotron U-400M is in a stage of build-up. GALS will apply the highly selective and efficient technique of stepwise resonant ionization in a gas cell (of the element of interest) with subsequent mass separation. The most efficient method to produce such nuclei, as motivated in [4], are the multi-nucleon transfer reactions. Our estimations show that at target thickness 0.3 mg/cm, ion beam of 0.1 pμA and setup efficiency of 10% we would be able to measure decay properties of 1 new isotope per day.

**References**

[1] Zagrebaev V I, Zemlyanoy S G, Kozulin E M, Kudryavtsev Yu, Fedosseev V, Bark R, Othman HA 2013 *Hyperfine Interact* **216,** 109
[2] Zagrebaev V I, Zemlyanoy S G, Kozulin E M *et al.* 2014 *Hyperfine Interact* **227,** 181
[3] Zagrebaev V I, Zemlyanoy S G, Kozulin E M *et al* 2016 *J. Phys.Conf. Series* Series **724,** 012057
[4] Zagrebaev V and Greiner W 2008 *Phys. Rev. Lett.* **101**, 122701
[5] Long Zh, Zhao-Qing Feng, Feng-Shou Zhang 2015 *J. Phys. G: Nucl. Part. Phys.* **42,** 085102
[6] Kurcewicz, J., Farinon, F., Geissel, H. et al. 2012 *Phys. Lett*. B **717** 371
[7] Kudryavstev Y *et al*. 2003 *Nucl. Instrum. Methods Phys. Res.* B **204**, 336
[8] Moore I D *et al* 2005 *J. Phys. G: Nucl. Part. Phys*. **31**, S1499
[9] Campbell P, Moore I D and Pearson M R 2016 *Prog. Particle Nucl. Phys.* **86,** 127
[10] Ravn H L and Allardyce B W 1989 In: *Treatise on Heavy-Ion Science*, **8**, 363
[11] Kazarinov N Yu 2016 *Physics of Particles and Nuclei Letters*, **13**, No. 7, 868
[12] Opera3D 2012 *Oxford OX5 1JE*, England
[13] Ferrer R *et al* 2013 *Nucl. Instrum. Methods Phys. Res*. B **317**, 570
[14] Kudryavtsev Y *et al* 2013 *Nucl. Instrum. Methods Phys*. Res. B **297**, 7
[15] http://simion.com/
[16] Traykov E (GANIL, CEA/DSM-CNRS/IN2P3, Caen, France) private communication
[17] Zemlyanoy S, Avvakumov A, Fedosseev V et al. 2017 *Hyperfine Interact* **238**, 31
[18] Karpov, A.V. EXON 2016 to be published
[19] Corliss, Charles H., Bozman, William R. Experimental transition probabilities for spectral lines of seventy elements, *NBS Monograph* **53** (1962)
[20] Meggers, William F. , Corliss, Charles H., Bourdon F. Scribner: Tables of spectral lines intensities (second edition), *NBS Monograph* **145** (1975)
[21] https://www.nist.gov/pml/atomic-spectra-database (version 5, updated October 2015)
[22] Sansonetti, J E, Martin W C 2005 *J. Phys. Chem. Reference Data* **34**, 1559
[23] Blum Joel D, Pellin M J, Calawa, W F et al. 1990 *Anal. Chem.* **62**, 209
[24] Calaway W F, Wien R C, Burnett D S et al. 1995 *J. Vac. Sci. Technol*. A **13**, 1310